RAPID COMMUNICATIONS

PHYSICAL REVIEW B **67**, 241301(R) (2003)

Noiseless scattering states in a chaotic cavity

P. G. Silvestrov,[1,2] M. C. Goorden,[1] and C. W. J. Beenakker[1]
[1]*Instituut Lorentz, Universiteit Leiden, P.O. Box 9506, 2300 RA Leiden, The Netherlands*
[2]*Budker Institute of Nuclear Physics, 630090 Novosibirsk, Russia*
(Received 11 February 2003; published 9 June 2003)

Shot noise in a chaotic cavity (Lyapunov exponent λ, level spacing δ, linear dimension L), coupled by two N-mode point contacts to electron reservoirs, is studied as a measure of the crossover from stochastic quantum transport to deterministic classical transport. The transition proceeds through the formation of *fully* transmitted or reflected scattering states, which we construct explicitly. The fully transmitted states contribute to the mean current $\bar{I}$, but not to the shot-noise power S. We find that these noiseless transmission channels do not exist for $N \lesssim \sqrt{k_F L}$, where we expect the random-matrix result $S/2e\bar{I} = 1/4$. For $N \gtrsim \sqrt{k_F L}$ we predict a suppression of the noise $\propto (k_F L/N^2)^{N\delta/\pi\hbar\lambda}$. This nonlinear contact dependence of the noise could help to distinguish ballistic chaotic scattering from random impurity scattering in quantum transport.

DOI: 10.1103/PhysRevB.67.241301 PACS number(s): 73.63.Kv, 05.45.Mt, 03.65.Sq, 72.70.+m

Shot noise can distinguish deterministic scattering, characteristic of particles, from stochastic scattering, characteristic of waves. Particle dynamics is deterministic. A given initial position and momentum fix the entire trajectory. In particular, they fix whether the particle will be transmitted or reflected, so the scattering is noiseless. Wave dynamics is stochastic. The quantum uncertainty in position and momentum introduces a probabilistic element into the dynamics, so it is noisy.

The suppression of shot noise in a conductor with deterministic scattering was predicted many years ago from this qualitative argument.[1] A better understanding, and a quantitative description, of how shot noise measures the transition from particle to wave dynamics in a chaotic quantum dot was put forward by Agam, Aleiner, and Larkin,[2] and developed further in Ref. 3. The key concept is the Ehrenfest time τ_E, which is the characteristic time scale of quantum chaos.[4] The noise power $S \propto \exp(-\tau_E/\tau_D)$ was predicted to vanish exponentially with the ratio of τ_E and the mean dwell time $\tau_D = \pi\hbar/N\delta$ in the quantum dot (with δ the level spacing and N the number of modes in each of the two point contacts through which the current is passed). A recent measurement of the N dependence of S is consistent with this prediction for $\tau_E < \tau_D$, although an alternative explanation in terms of short-range impurity scattering describes the data equally well.[5]

The theory of Ref. 2 introduces the stochastic element by means of long-range impurity scattering, and adjusts the scattering rate so as to mimic the effect of a finite Ehrenfest time. Here we take the alternative approach of explicitly constructing noiseless channels in a chaotic quantum dot. These are scattering states which are either fully transmitted or fully reflected in the semiclassical limit. They are not described by random matrix theory.[6] By determining what fraction of the available channels is noiseless, we can deduce a precise upper bound for the shot-noise power. A random matrix conjecture for the remaining noisy channels gives an explicit form of $S(N)$. We find that the onset of the classical suppression of the noise is described not only by the Ehrenfest time, but by the difference of τ_E and the ergodic time τ_0, which we introduce and calculate in this Rapid Communication. The resulting nonlinear dependence of $\ln S$ on N may help to distinguish between the competing explanations of the experimental data.[5]

We illustrate the construction of noiseless scattering states for the two-dimensional billiard with smooth confining potential $U(x,y)$ shown in Fig. 1. The outer equipotential defines the area in the x-y plane which is classically accessible at the Fermi energy $E_F = p_F^2/2m$ (with $p_F = \hbar k_F$ the Fermi momentum). The motion in the closed billiard is chaotic, with a Lyapunov exponent λ. We assume the billiard to be connected at $x=0$ and $x=L$ by two similar point contacts to leads of width W extended along the $\pm x$ direction.

The beam of electrons injected through a point contact into the billiard has a cross section W and transverse momenta in the range $(-p_W, p_W)$. The number of channels $N \simeq p_W W/\hbar$ in the lead is much smaller than the number of

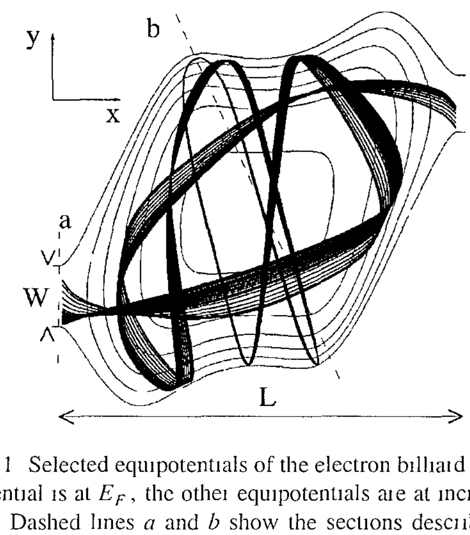

FIG. 1. Selected equipotentials of the electron billiard. The outer equipotential is at E_F, the other equipotentials are at increments of $0.19E_F$. Dashed lines a and b show the sections described in the text. Also shown is a flux tube of transmitted trajectories all originating from a single closed contour in a transmission band representing the spatial extension of a fully transmitted scattering state. The flux tube is wide at the two openings and squeezed inside the billiard.

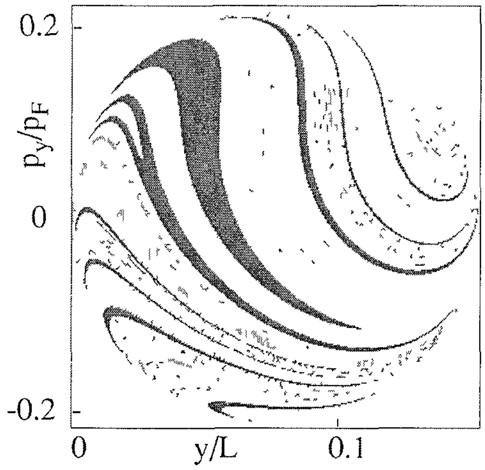

FIG 2. Section of phase space at $p_x=\sqrt{p_F^2-p_y^2}$ and $x=0$, corresponding to line a in Fig 1. Each dot in this surface of section is the starting point of a classical trajectory that is transmitted through the lead at $x=L$ (black/red), or reflected back through $x=0$ (gray/green) The points lie in narrow bands Only the trajectories with dwell time $t<12mL/p_F$ are shown.

channels $M\simeq p_F L/\hbar$ supported by a typical cross section of the billiard. While $W/L\ll 1$ in general, the ratio p_W/p_F depends on details of the potential near the point contact. If $p_W/p_F\ll 1$ one speaks of a collimated beam. This is typical for a smooth potential, while a hard-wall potential typically has $p_W\simeq p_F$ (no collimation). We define $r_{\min}=\min(W/L,p_W/p_F)$ and $r_{\max}=\max(W/L,p_W/p_F)$.

The classical phase space is four dimensional. By restricting the energy to E_F and taking $x=0$ we obtain the two-dimensional section of phase space shown in Fig. 2. The accessible values of y and p_y lie in a disc-shaped region of area $\mathcal{A}=Nh$ in this surface of section. Up to factors of order unity, the disk has width $r_{\min}$ and length $r_{\max}$ (if coordinate and momentum are measured in units of L and p_F, respectively). In Fig. 2 one has $r_{\min}\simeq r_{\max}$. Each point in the disc defines a classical trajectory that enters the billiard (for positive p_x) and then leaves the billiard either through the same lead (reflection) or through the other lead (transmission). The points lie in narrow bands, which we will refer to as "transmission bands" and "reflection bands."

It is evident from Fig. 2 that the area A_j enclosed by a typical transmission (or reflection) band j is much less than $\mathcal{A}$. For an estimate we consider the time $t(y,p_y)$ that elapses before transmission. Let t_j be the dwell time averaged over the starting points y, p_y in a single band. The fluctuations of t around the average are of the order of the time $t_W\simeq mW/p_W$ to cross the point contact, which is typically $\ll t_j$. As we will see below, the area of the band decreases with t_j as

$$A_j\simeq\mathcal{A}_0\exp(-\lambda t_j)\quad\text{if } t_j\gg 1/\lambda,t_W. \tag{1}$$

The prefactor $\mathcal{A}_0=\mathcal{A}r_{\min}/r_{\max}$ depends on the degree of collimation. In Ref. 7 the symmetric case $r_{\min}=r_{\max}$ was assumed, when $\mathcal{A}_0=\mathcal{A}$.

We now proceed to the construction of fully transmitted scattering states. To this end we consider a closed contour C within a transmission band j. The starting points on the contour define a family of trajectories that form a flux tube inside the billiard (see Fig. 1). The semiclassical wave function

$$\psi(x,y)=\sum_\sigma \sqrt{\rho_\sigma(x,y)}\exp[iS_\sigma(x,y)/\hbar] \tag{2}$$

is determined as usual from the action S_σ and density ρ_σ that solve the Hamilton-Jacobi and continuity equations

$$|\nabla S|^2=2m(E_F-U),\quad \nabla\cdot(\rho\nabla S)=0. \tag{3}$$

The action is multivalued and the index σ labels the different sheets. Typically, there are two sheets, one originating from the upper half of the contour C and one from the lower half.

The requirement that ψ is single valued as one winds around the contour imposes a quantization condition on the enclosed area,

$$\oint_C p_y dy=(n+1/2)h. \tag{4}$$

The increment 1/2 accounts for the phase shift acquired at the two turning points on the contour. The quantum number $n=0,1,2,\ldots$ is the channel index. The largest value of n occurs for a contour enclosing an area A_j. The number of transmission channels N_j within band j is therefore given by A_j/h, with an accuracy of order unity. In view of Eq. (1) we have

$$N_j\simeq(\mathcal{A}_0/h)\exp(-\lambda t_j)\quad\text{for } t_j<\tau_E, \tag{5a}$$

$$N_j=0\quad\text{for } t_j>\tau_E. \tag{5b}$$

The time

$$\tau_E=\lambda^{-1}\ln(\mathcal{A}_0/h)=\lambda^{-1}\ln(Nr_{\min}/r_{\max}), \tag{6}$$

above which there are no fully transmitted channels, is the Ehrenfest time of this problem.

By decomposing one of these N_j scattering states into a given basis of transverse modes in the lead one constructs an eigenvector of the transmission matrix product $tt^\dagger$. The corresponding eigenvalue $T_{j,n}$ is equal to unity with exponential accuracy in the semiclassical limit $n\gg 1$. Because of the degeneracy of this eigenvalue any linear combination of eigenvectors is again an eigenvector. This manifests itself in our construction as an arbitrariness in the choice of C.

We observe in Fig. 1 that the spatial density profile $\rho(x,y)$ of a fully transmitted scattering state is highly nonuniform. The flux tube is broad (width of order W) at the two openings, but is squeezed down to very small width inside the billiard. A similar effect was noted[7] in the excited states of an Andreev billiard (a cavity connected to a superconductor). Following the same argument we estimate the minimal width of the flux tube as $W_{\min}\simeq L\sqrt{N_j/k_F L}$.

The total number

$$N_0=\sum_j N_j=N\int_0^{\tau_j} P(t)dt \tag{7}$$

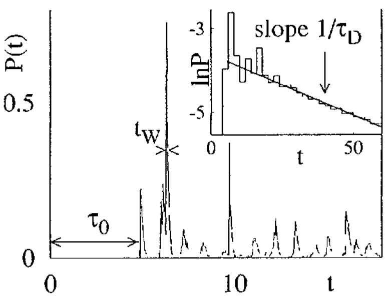

FIG. 3. Dwell-time distribution for the billiard of Fig. 1. Electrons at the Fermi energy are injected through the left lead. Time is in units of mL/p_F. Inset: the same data on a semilogarithmic scale with larger bin size of the histogram. Three characteristic time scales are seen: t_W, τ_0, and τ_D.

of fully transmitted and reflected channels is determined by the dwell-time distribution $P(t)$.[8] Figure 3 shows this distribution in our billiard. One sees three different time scales. The narrow peaks represent individual transmission (reflection) bands. They consist of an abrupt jump followed by an exponential decay with a time constant t_W. These exponential tails correspond to the borders of the bands, where the trajectory bounces many times between the sides of the point contact. If we smooth $P(t)$ over such short time intervals, an exponential decay with time constant $\tau_D = \pi\hbar/N\delta$ is obtained (inset). The decay starts at the so called "ergodic time" τ_0. There are no trajectories leaving the cavity for $t < \tau_0$. So the smoothed dwell-time distribution has the form

$$P(t) = \tau_D^{-1}\exp[(\tau_0 - t)/\tau_D]\theta(t-\tau_0), \tag{8}$$

with $\theta(t)$ the unit step function.

In order to find τ_0 we consider Fig. 4, where the section of phase space along a cut through the middle of the billiard is shown (line b in Fig. 1). It is convenient to measure the momentum and coordinate along b in units of p_F and L. The

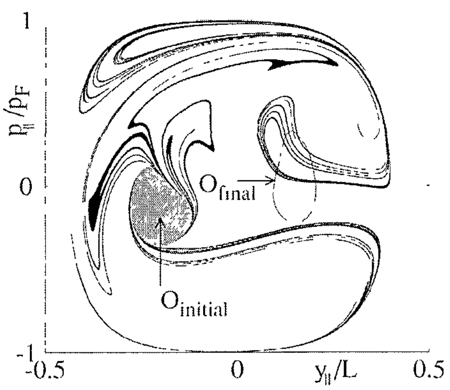

FIG. 4. Section of phase space in the middle of the billiard, along line b in Fig. 1. The subscript $\|$ indicates the component of coordinate and momentum along this line. Elongated black areas O_j show the positions of the fifth crossing of the injected beam with this surface of section. The area $O_{\rm initial}$ is the position of the first crossing. Points inside $O_{\rm final}$ leave the billiard without further crossing of line b. For times less than the ergodic time τ_0 there is no intersection between O_j and $O_{\rm final}$.

injected beam crosses the section for the first time over an area $O_{\rm initial}$ of size $r_{\rm max}\times r_{\rm min} = hN/p_F L$. (Fig. 4 has $r_{\rm min} \simeq r_{\rm max}$, but the estimates hold for any $r_{\rm min} < r_{\rm max} < 1$.) Further crossings consist of increasingly more elongated areas. The fifth crossing is shown in Fig. 4. The flux tube intersects line b in a few disjunct areas O_j, of width $r_{\rm min}e^{-\lambda t}$ and total length $r_{\rm max}e^{\lambda t}$. (Due to conservation of the integral $\oint \mathbf{p}\cdot d\mathbf{r}$ enclosing the flux tube, the total area $\Sigma_j O_j$ decreases only when particles leave the billiard.) The typical separation of adjacent areas is $(r_{\rm max}e^{\lambda t})^{-1}$. To leave the billiard (through the right contact) without a further crossing of b a particle should pass through an area $O_{\rm final} \simeq r_{\rm max}\times r_{\rm min}$. This is highly improbable[9] until the separation of the areas O_j becomes of order $r_{\rm max}$, leading to the ergodic time

$$\tau_0 = \lambda^{-1}\ln r_{\rm max}^{-2}. \tag{9}$$

The ergodic time varies from $\tau_0 \lesssim \lambda^{-1}$ for $r_{\rm max} \simeq 1$ to $\tau_0 = \lambda^{-1}\ln(k_F L/N)$ for $r_{\rm min} \simeq r_{\rm max}$. The overlap of the areas O_j and $O_{\rm final}$ is the mapping of the transmission band onto the surface of section b. It has an area $p_F L r_{\rm min}^2 e^{-\lambda t} = \mathcal{A}(r_{\rm min}/r_{\rm max})e^{-\lambda t}$, leading to Eq. (1).

Substituting Eq. (8) into Eq. (7) we arrive at the number N_0 of fully transmitted and reflected channels:

$$N_0 = N\theta(\tau_E - \tau_0)[1 - e^{(\tau_0-\tau_E)/\tau_D}], \tag{10}$$

$$\tau_E - \tau_0 = \lambda^{-1}\ln(N^2/k_F L). \tag{11}$$

There are no fully transmitted or reflected channels if $\tau_E < \tau_0$, and hence if $N < \sqrt{k_F L}$. Notice that the dependence of τ_E and τ_0 separately on the degree of collimation drops out of the difference $\tau_E - \tau_0$. The number of noiseless channels is therefore insensitive to details of the confining potential. An Ehrenfest time $\propto \ln(N^2/k_F L)$ has appeared before in connection with the Andreev billiard,[10] but the role of collimation (and the associated finite ergodic time) was not considered there.

Equations (5) and (8) imply that the majority of noiseless channels group in bands having $N_j \gg 1$, which justifies the semiclassical approximation. The total number of these noiseless bands is $(N-N_0)/\lambda\tau_D$, which is much less than both $N-N_0$ and N_0. Because of this inequality the relatively short trajectories contributing to the noiseless channels are well separated in phase space from other, longer trajectories (cf. Fig. 2).

The shot-noise power S is related to the transmission eigenvalues by[11]

$$S = 2e\bar{I}g^{-1}\sum_{k=1}^{N}\mathcal{T}_k(1-\mathcal{T}_k), \tag{12}$$

with $\bar{I}$ the time-averaged current and $g = \Sigma_k \mathcal{T}_k$ the dimensionless conductance. The N_0 fully transmitted or reflected channels have $\mathcal{T}_k = 1$ or 0, hence they do not contribute to the noise. The remaining $N-N_0$ channels contribute at most 1/4 per channel to $Sg/2e\bar{I}$. Using that $g = N/2$ for large N, we arrive at an upper bound for the noise power $S < e\bar{I}(1 - N_0/N)$.

For a more quantitative description of the noise power we need to know the distribution $P(\mathcal{T})$ of the transmission eigenvalues for the $N-N_0$ noisy channels, which cannot be described semiclassically. We expect the distribution to have the same bimodal form $P(\mathcal{T})=\pi^{-1}\mathcal{T}^{-1/2}(1-\mathcal{T})^{-1/2}$ as in the case $N_0=0$.[6] This expectation is motivated by the earlier observation that the N_0 noiseless channels are well separated in phase space from the $N-N_0$ noisy ones. Using this form of $P(\mathcal{T})$ we find that the contribution to $Sg/2e\bar{I}$ per noisy channel equals $\int_0^1\mathcal{T}(1-\mathcal{T})P(\mathcal{T})d\mathcal{T}=1/8$, half the maximum value. The Fano factor $F=S/2e\bar{I}$ is thus estimated as

$$F=\frac{1}{4}\quad \text{for } N\lesssim\sqrt{k_FL}, \tag{13a}$$

$$F=\frac{1}{4}(k_FL/N^2)^{N\delta/\pi\hbar\lambda}\quad \text{for } N\gtrsim\sqrt{k_FL}. \tag{13b}$$

This result should be compared with that of Ref. 2: $F'=\frac{1}{4}(k_FL)^{-N\delta/\pi\hbar\lambda}$. The ratio $F'/F=\exp[(2N\delta/\pi\hbar\lambda)\ln(N/k_FL)]$ is always close to unity (because $N\delta/\pi\hbar\lambda\simeq N/k_FL\ll 1$). But $F-\frac{1}{4}$ and $F'-\frac{1}{4}$ are entirely different for $N\lesssim\sqrt{k_FL}$, which is the relevant regime in the experiment.[5] There the N dependence of the shot noise was fitted as $F=\frac{1}{4}(1-t_Q/\tau_D)=\frac{1}{4}(1-\text{const}\times N)$, where t_Q is some N-independent time. Equation (13) predicts a more complex N dependence, a plateau followed by a decrease as $\ln F\propto -N\ln(N^2/k_FL)$, which could be observable if the experiment extends over a larger range of N.

We mention two other experimentally observable features of the theory presented here. The reduction of the Fano factor described by Eq. (13) is the cumulative effect of many noiseless bands. The appearance of new bands with increasing N introduces a fine structure in $F(N)$, consisting of a series of cusps with a square-root singularity near the cusp. The second feature is the highly nonuniform spatial extension of open channels, evident in Fig. 1, which could be observed with the scanning tunneling microscopy technique of Ref. 12. From a more general perspective the noiseless channels constructed in this paper show that the random matrix approach may be used in ballistic systems only for sufficiently small openings: $N\lesssim\sqrt{k_FL}$ is required. For larger N the scattering becomes deterministic, rather than stochastic, and random matrix theory starts to break down.

This work was supported by the Dutch Science Foundation NWO/FOM.

[1] C. W. J. Beenakker and H. van Houten, Phys. Rev. B 43, 12 066 (1991).

[2] O. Agam, I. Aleiner, and A. Larkin, Phys. Rev. Lett. 85, 3153 (2000).

[3] H.-S. Sim, and H. Schomerus, Phys. Rev. Lett. 89, 066801 (2002); R. G. Nazmitdinov, H. S. Sim, H. Schomerus, and I. Rotter, Phys. Rev. B 66, 241302(R) (2002).

[4] G. M. Zaslavsky, Phys. Rep. 80, 157 (1981).

[5] S. Oberholzer, E. V. Sukhorukov, and C. Schonenberger, Nature (London) 415, 765 (2002).

[6] R. A. Jalabert, J.-L. Pichard, and C. W. J. Beenakker, Europhys. Lett. 27, 255 (1994).

[7] P. G. Silvestrov, M. C. Goorden, and C. W. J. Beenakker, Phys. Rev. Lett. 90, 116801 (2003).

[8] The dwell-time distribution is defined with a uniform measure in the surface of section of the lead, so that its integral is directly proportional to the number of channels. The mean dwell time $\tau_D=\pi\hbar/N\delta$ was calculated by W. Bauer and G. F. Bertsch, Phys. Rev. Lett. 65, 2213 (1990).

[9] Dwell times shorter than τ_0 are improbable but they may exist for special positions of the two point contacts. The probability that a random position permits a transmitted (or reflected) trajectory of duration $t<\tau_0$ is $\exp[-\lambda(\tau_0-t)]$.

[10] M. G. Vavilov and A. I. Larkin, Phys. Rev. B 67, 115335 (2003).

[11] M. Buttiker, Phys. Rev. Lett. 65, 2901 (1990).

[12] M. A. Topinka *et al.*, Nature (London) 410, 183 (2001).